

Natural Extracts-mediated Biosynthesis of Zinc Oxide Nanoparticles and Their Multiple Pharmacotherapeutic Perspectives

A. G. M. Haldar^a, D. Kar Mahapatra^b, K. M. Dadure^c and R. G. Chaudhary^d

^aDepartment of Applied Chemistry, Priyadarshini Bhagwati College of Engineering, Nagpur 440009, Maharashtra, India.

^bDepartment of Pharmaceutical Chemistry, Dadasaheb Balpande College of Pharmacy, Nagpur 440037, Maharashtra, India.

^cDepartment of Chemistry, J. B. College of Science, Wardha 442001, Maharashtra, India.

^dPost-graduate Department of Chemistry, S. K. Porwal College, Kamptee, Nagpur 441001, Maharashtra, India.

Doi: <https://doi.org/10.47011/15.1.10>

Received on: 01/08/2020;

Accepted on: 01/09/2021

Abstract: Eco-friendly green syntheses of nanoparticles (NPs) have involved the natural biomass contents since over a decade. The NPs of zinc oxide (ZnO) have important applications in diagnostics, detection of biomolecules, opto-electronic devices, microelectronics like electromagnetic coupled sensor laser devices, neutralization of environmental hazard pollutants as well as pharmaceutical components from water. ZnO-NPs play a pivotal role in drug delivery, exhibiting biomedical activities, such as anti-pathogenics, diagnosis of various diseases, anti-oxidants etc. The interest in synthesizing ZnO-NPs *via* the biological method (plant extracts) has increased considerably in the last few decades. The development of this new approach and the significant interest in it are mainly related to the absence of toxic chemicals or high-energy applied methods to the biological synthesis which develop more environmentally friendly and cost-effective methods. This review article focuses on recent (January 2020 to May 2020) plant-mediated green synthetic methods which are highlighted comprehensively in this review article.

Keywords: Zinc, Nanoparticles, Natural, Synthesis, Plant, Extract.

Introduction

Nanotechnology has been a subject of great research and enthusiasm for researchers in recent years [1]. Nanomaterials having nanoscale dimensions possess unique properties as compared to their micro-molecules. The most current approach focuses on more cost-effective techniques for creating and manipulating materials at the nanometer scale [2]. The research on nanomaterials is one of the most demanding and greatly growing areas in the branch of science and engineering. Nanoparticles (NPs) of different noble metals have been

already in practice for therapeutic purposes since centuries ago. These NPs proved to be very valuable for pharmaceutical, biomedical and tissue engineering [3].

Synthesis of NPs is conducted by biological or green technology and physical and chemical methods. The two end processes of developing NPs have been accompanied by costly and environmentally hazardous effects. In chemical synthesis, toxic and hazardous chemicals are involved in NP synthesis, which causes various ecological risks and serious diseases.

Pharmacological importance of zinc oxide (ZnO) nanoparticles has been studied for their unique characteristics [4]. Due to the large surface area of the ZnO-NPs, they are used to remove hazardous chemicals, like chromium and lead from effluents [5], as well as hazardous components from radioactive effluents [6]. The nanoparticles of ZnO have important applications in diagnostics, detection of biomolecules, opto-electronic devices, microelectronics like electromagnetic coupled sensor laser devices [7], neutralization of environmental hazard pollutants as well as pharmaceutical components from water [8-10]. In the area of pharmacological research, ZnO-NPs play a pivotal role in drug delivery, exhibiting biomedical activities, such as anti-pathogenics, diagnosis of various diseases, anti-oxidant, ... etc. These NPs of ZnO are very prominent against pathogenic species such as *E. coli*, *Salmonella*, *S. aureus* and *B. subtilis* using different susceptibility test protocols, as has been reported [11].

Plausible Mechanism(s) of ZnO Nanoparticle Formation

Eco-friendly green syntheses of NPs have involved the plant contents since over a decade. Since the early twentieth century, it has been found out that the plant extracts have the capability to reduce metal ions to their reduced form. This has come in the limelight of experimental form only a few decades ago for the reduction of metal salts. The different bioactive molecules, like phenols, alkaloids, citric acid, terpenes, polyphenolic, flavonoids, ascorbic acid, and many more present in the plant extract, play an important role as reducing agents. The biosynthesis of nanoparticles through plant biomass is very important in the field of nanotechnology, because the plant extract acts as both a capping and a reducing agent. The development of this new approach and the significant interest in it are mainly related to the absence of toxic chemicals or high-energy applied methods to the biological synthesis, which develop methods that are more environmentally friendly and cost-effective. The plant-oriented mechanism involves an intracellular and an extracellular pathway to synthesize the nanoparticles. In the intracellular pathway, the metals are absorbed through the roots by utilizing growing media of plant with the metal-rich organic component, metal-

enriched soil and hydroponic solution with high metal contamination [12-15]. The extracellular pathway involved the synthesis of NPs by using the extracts (by boiling and crushing) of different parts of the plants (Fig. 1) [16].

Plant-mediated Biosynthesis of ZnO Nanoparticles and Their Applications

In the last several decades, there has been a surge in interest in biologically manufacturing ZnO-NPs. Literature indicates that the biosynthesis of metal oxides or reduced to metallic NPs is more eco-friendly than the conventional physicochemical methods used presently. These fabricated ZnO-NPs of varied shapes, like spherical, hexagonal, quasi-spherical, rod, ... etc. demonstrate diverse pharmacological applications ranging from anti-fungal (*Alternaria mali*, *Aspergillus fumigatus*, *Aspergillus niger*, *Candida albicans*), anti-bacterial (*Bacillus pumilus*, *Bacillus subtilis*, *Escherichia coli*, *Pseudomonas aeruginosa*, *Salmonella typhi*, *Staphylococcus aureus*, and *Vibrio cholera*), anti-nociceptive, anti-proliferative, anti-mitotic, anti-inflammatory, anti-diabetic, anti-leishmanial, osteoclast inhibition, anti-oxidant, dressing element, local anesthetics, muscle relaxants, ... etc. The plant-mediated green synthetic methods or biological methods are highlighted comprehensively.

Anti-microbial Applications of ZnO-NPs

Sara Zafar *et al.* have synthesized eco-friendly ZnO-NPs by utilizing $ZnSO_4 \cdot 7H_2O$ with the help of aqueous extract of seeds of sesame. They have developed spherical-shaped 9.07 nm particles of ZnO. The anti-bacterial activity of newly synthesized Zn-NPs possesses greater values against various bacteria compared to the std. gentamicin. The zone of inhibition produced by Zn-NPs against various strains of Bacteria is: *P.aeruginosa* (12.6mm), *E.coli* (10.4mm), *S.pneumonia* (8.6 mm) and *S.aureu* (4.1mm) with respect to 120 μ g/l [17].

Velsankar *et al.* conducted an experiment to prepare cost-effective and environment-friendly ZnO-NPs by biogenic reduction of $Zn(CH_3COO)_2 \cdot 2H_2O$ through deionized water and ethanol mixed extract of grain powder of *Echinochloa frumentacea* which produced nanoparticles of hexagonal shape and size of 35-85 nm. The antibacterial activity of ZnO-NPs has a higher antibacterial effect against *Bacillus pumilus* and *Salmonella typhi* than a standard

drug of ciprofloxacin. Results showed that the zone of inhibition rate was perceived at 18, 20, 23, 24, 26 and 29 mm (against *Bacillus pumilus* bacterium) and at 13, 16, 18, 21, 25 and 27 mm (against *Salmonella typhi* bacterium) for 25, 50, 100, 250, 500 and 1000 µg/mL concentrations, respectively. Nature of the diversity in the cell wall structure is responsible for different zones of inhibition rate against *Bacillus pumilis* and *Salmonella typhi* [18].

Ahmad *et al.* have studied the green synthesis of ZnO-NPs with the help of *Euphorbia hirta* leaves extract which acted as a reducing and capping agent with zinc nitrate ($Zn(NO_3)_2$) as a precursor of the reaction. The newly formed ZnO-NPs have a spherical shape with 20-25 nm size. The antibacterial study of synthesized nanoparticles clearly revealed that the zone of inhibition increases with increasing the conc. of ZnO-NPs (20-100 mg/ml), which may be due to the increase of H_2O_2 concentration from the surface of ZnO-NPs. In measuring zone of inhibition, *Streptococcus aureus* (29 mm) was found to be highest when compared to other bacteria, like *Streptococcus mutans* (28 mm), *Clostridium absonum* (27 mm), *Escherichia coli* (24 mm) against the std. drug streptomycin which was used as a control [19].

Di *et al.* have reported the biosynthesis of ZnO-NPs by treating radish root (*Raphanus sativus*) extract with zinc acetate dihydrate [$Zn(CH_3COO)_2 \cdot 2H_2O$] as the initiator of the reaction. The reported NPs have hexagonal-shaped morphology with 15-25 nm size. Antibacterial property of synthesized ZnO-NPs, displayed on multidrug-resistant bacteria along with ATCC microbial strains, correlated with the zone of inhibition (mm). MDR-*Staphylococcus aureus* showed highest zone of inhibition (21.23 ± 1.16 mm) and *S.aureus* ATCC 29213 showed an inhibition zone of (21.32 ± 1.53 mm) when compared with ZnO-NPs and plant extract. Lowest zone of inhibition was observed by *E.faecalis* ATCC 29212 (11.23 ± 0.58 mm). Excellent antibacterial activity towards microbes isolated from diabetic foot ulcers, like *P.aeruginosa* ATCC 27853, MDR-*E.coli*, *S.aureus* ATCC 29213, MDR-MRSA, *E.coli* ATCC 25922, *E.faecalis* ATCC 29212, MDR-*P.aeruginosa* and MDR-*A.baumannii*, was shown using the disc diffusion method [20].

Fahimmunisha *et al.* have revealed an interesting fact regarding flora-mediated

synthesis of ZnO-NPs employing an aqueous extract of *Aloe socotrina* leaf by utilizing zinc acetate dihydrate as the precursor. The spherical-shaped NPs of 15-50 nm size exhibited interesting pharmacological activity. The antibacterial action showed that *Aloe socotrina*(As)-ZnO-NPs had dynamic dose-dependent activity against UTI pathogens, such as *Escherichia coli*, *Klebsiella pneumonia*, *Proteus vulgaris* (HQ640434), *Pseudomonas aeruginosa* (ATCC) and the maximum zone of inhibition was shown against *E. coli* (19.2 ± 0.8 mm) and *P. vulgaris* (25.0 ± 0.9 mm). The As extract and As-ZnO-NPs showed bacteriostatic activity against *Proteus vulgaris* and *Pseudomonas aeruginosa* at low concentrations of 75 µg/mL and 50 µg/mL, respectively. The synthesized ZnO nanoparticles have anti-biofilm properties [21].

Maruthupandy *et al.* have synthesized eco-friendly ZnO-NPs by utilizing zinc nitrate hexahydrate [$Zn(NO_3)_2 \cdot 6H_2O$] and reducing it with the help of aqueous extract of *Camellia japonica* leaf. The synthesized NPs were spherical-shaped and 15-30 nm in size. The antibacterial activity of ZnO-NPs against gram-positive bacteria was found to be 21mm and 11.5mm for *S. pneumoniae* and *B. subtilis* at 100 µg/mL concentration, respectively. The NPs showed better activity at 100 µg/mL concentration against gram-negative bacteria with zone of inhibition of 10.5, 18 mm and 11, 12 mm for *E. coli* and *S. typhimurium*, respectively. The size of inhibition zone was concentration-dependent of ZnO-NPs. The results revealed that the sensitivity of *S. pneumoniae* was higher at the lowest concentration of ZnO-NPs. The maximum zone of inhibition of *S. pneumoniae* (21 mm) was higher at the highest concentration of ZnO-NPs when compared to other pathogens [22].

Rasli *et al.* have reported the fresh *Aloe vera* leaf-mediated ZnO-NPs with the help of aqueous extract by utilization of zinc nitrate used as the precursor. The research revealed the fabrication of rod-shaped 16-nm NPs. The antibacterial action was measured by the active inhibition zone around 1.325mm^2 against *E. Coli* after 24 h of incubation. The inhibition zone clearly indicates that membrane disruption leads to the death of pathogens. ZnO is a well-known antibacterial agent and is effective at very low

concentration of bacteria as compared to the standard [23].

Mydeen *et al.* synthesized ZnO-NPs from the precursor zinc acetate dihydrate through an eco-friendly approach utilizing the aqueous extract of *Prosopis juliflora* leaf. The spherically shaped NPs of 83 nm size demonstrated notable anti-pathogenic activities. The antibacterial activities have been carried out (*in vitro*) against four different pathogens viz *E.coli*, *R. rhodochrous*, *B. subtilis* and *V.cholera* against streptomycin sulfate as standard. A higher zone of inhibition of 25 mm was perceived in the gram-negative bacteria *V.cholera* similar to other gram-positive bacterial strains. Observations concluded that the synthesized ZnO-NPs had an antibacterial character confirmed by clear zone of inhibition representing biocidal behavior. They were distributed in the bacterial membranes and the formation of surface oxygen species from ZnO led to bacterial cell death [24].

Uma *et al.* have studied the potentials of flora-mediated synthesis of ZnO-NPs by reducing the precursor zinc acetate with aqueous extract of fresh plum fruits. From antibacterial activity of ZnO-NPs, it can be inferred that the growth of bacterial cells was lower than that of cells in the control, indicating that ZnO-NPs could inhibit the growth of bacterial cells. The percentage of bacterial growth decreased to 5.1-100% for *E.coli* and 23.43-99.48% for *S.aureus*, respectively. Maximum and minimum growth reduction was at 80 ppm and 20 ppm, respectively. Results concluded that *S.aureus*, being the gram-positive bacteria having single peptidoglycan layer, seemed to be more sensitive to the ZnO-NPs as compared to the *E.coli* having two outer membranes; i.e., peptidoglycan and outer lipid membrane. There was a sharp reduction in the growth of *S.aureus* with the increase in concentration of ZnO-NPs [25].

Awwad *et al.* applied an eco-friendly aqueous extract of *Ailanthus altissima* fruits and synthesized spherical-shaped ZnO-NPs of size 5-18 nm from the precursor zinc nitrate hexahydrate $[Zn(NO_3)_2 \cdot 6H_2O]$. Antibacterial activity of synthesized ZnO-NPs was tested on gram-negative bacteria *E.coli* and gram-positive bacteria *S.aureus*. As the concentration of ZnO-NPs increases, the zone of inhibition also increases against the bacteria strains. ZnO-NPs (0.5mg/ml) have a significant growth inhibition effect against *S.aureus* and *E.coli* bacteria. This

effect is due to high surface area of ZnO-NPs and their small particle size of 12 nm. ZnO-NPs performed antimicrobial activities when tested against *Staphylococcus aureus*, *Bacillus subtilis*, *Proteus vulgaris*, *Pseudomonas aeruginosa*, *Candida albicans* and *Aspergillus niger* and gave good inhibition results [26].

Ansari *et al.* revealed the interesting potentials of flora-mediated synthesis of ZnO-NPs from an aqueous extract of *Cinnamomum verum* by utilizing $[Zn(NO_3)_2 \cdot 6H_2O]$ as the precursor. The synthesized spherical NPs of 45-nm size showed promising antibacterial activity. The green synthesized ZnO-NPs showed significant inhibition against the test pathogens (*S.aureus* and *E.coli*) compared to the control. ZnO-NPs offered a maximum zone of inhibition of 16.75 mm and 13.25 mm observed against *S.aureus* and *E.coli*, respectively. Observations resulted in that the gram-positive (*S.aureus*) bacteria showed to be more sensitive to the green synthesized ZnO-NPs compared to the gram-negative (*E.coli*) bacteria. The green synthesized ZnO-NPs inhibited the growth of *E.coli* and *S.aureus* with an MIC of 125 μ g/mL and 62.5 μ g/mL, respectively. The results concluded that the synthesized ZnO-NPs can be used as a potential antimicrobial agent against harmful pathogens [27].

Ahmad *et al.* have designed and synthesized environmentally friendly originated ZnO spherical NPs of size 52-70 nm from the aqua extract of *Eucalyptus globules* leaf by utilizing zinc nitrate hexahydrate $[Zn(NO_3)_2 \cdot 6H_2O]$ as the precursor. The aqueous broth was observed to be an efficient reducing agent, leading to the rapid formation of ZnNPs of varied shapes with sizes ranging between 52–70 nm. In addition, antifungal activity of the biosynthesized ZnNPs was evaluated against major phytopathogens of apple orchards. The fungal growth inhibition rate was found to be 76.7% for *Alternaria mali*, followed by 65.4 and 55.2% inhibition rate for *Botryosphaeria dothidea* and *Diplodia seriata*, for 100ppm of ZnNPs, respectively [28].

Anti-diabetic Applications of ZnO-NPs

Bayrami *et al.* have synthesized eco-friendly ZnO-NPs by utilizing $[Zn(NO_3)_2 \cdot 6H_2O]$ as a precursor with the aid of aqueous leaf extract of nettle (*Urtica dioica*). The antidiabetic activity of ZnO and ZnO-extract samples was examined through injection to alloxan-diabetic rats for a period of 16 days. The levels of insulin, FBS,

TG, TC and HDLC were measured in the blood serums of the treated rats before and after treatment. A statistical comparison was carried out for the level of insulin in rats suffering from diabetes, prior to and following the treatment. The level of insulin in non-diabetic healthy rats was 1.66 mg/L. This level was significantly reduced to 0.6 mg/L in rats with diabetes [29].

Anti-nociception Applications of ZnO-NPs

Xu *et al.* have reported the biosynthesis of ZnO-NPs with the help of deionized water extract of fresh leaves of *Selaginella convolute* by utilization of the precursor zinc acetate for bioreduction. This research highlighted the formation of spherical-shaped 40-nm ZnO-NPs. The ZnO-NPs and *S.convolute* extract possess an important antinociceptive operation (where $P < 0.001$) at the studied concentrations. For both ZnO-NPs as well as *S.convolute* extract, they have a dose-dependent impact. The percentage of *S.convolute* extract analgesic impact at 50 mg/kg was 66.45%, whereas at 100 mg/kg, it was 78.98%. Likewise, at levels of 5 and 10 mg/kg, the percentage of acetic acid attenuation caused writhes for ZnO-NPs of 72.87 and 80.76 %. The muscle relaxant impact of ZnO-NPs as well as *S.convolute* extract resulted in that post 20 min of administration, *S.convolute* extract at 50 and 100 mg/kg generated an important muscle relaxant activity (where $P < 0.05$) in both the traction and chimney studies. In the traction study, ZnO-NPs showed equally important (where $P < 0.05$) muscle relaxant impacts at 5 and 10 mg/kg, but the impact was noticed to be more pronounced in the chimney experiment at 10 mg/kg (where $P < 0.01$). The normal 0.25 mg/kg injection of diazepam generated an important muscle relaxant activity (where $P < 0.01$) in both studies [30].

Wang *et al.* have synthesized eco-friendly approach-based ZnO-NPs from $Zn(CH_3COO)_2 \cdot 2H_2O$ with the help of aqueous extract of *Fraxinus rhynchophylla* wood. The ecosynthesized ZnO-NPs of 100-200 nm size were assessed for anti-nociceptive property by using different models. The sedative effect of synthesized ZnO-NPs was evaluated with an open field test. Results of both thermal stress-induced methods (hot-plate and tail-immersion nociception tests) verified that the synthesized ZnO nanoparticles are a potent antinociceptive drug. ZnO nanoparticles effectively reduced the abdominal writhes in acetic acid-induced

nociception and significantly decreased the nociception activity in other glutamate-, capsaicin- and formalin-induced nociception models. Open-field experiment proved that synthesized ZnO nanoparticles are less sedative compared to the standard antinociceptive drug morphine [31].

Wound Healing Applications of ZnO-NPs

Zhang *et al.* have reported the plant-mediated synthesis of ZnO-NPs by using *Allium saralicum* R.M. Fritsch leaf extract with zinc nitrate hexahydrate $Zn(NO_3)_2 \cdot 6H_2O$ as the initiator of the reaction. The reported spherical-shaped NPs have 19 nm of average size. In search of wound healing effects of zinc nitrate, *A.saralicum*(As) and ZnNPs-As, 0.2% ointments were formulated and compared with the control and untreated groups. The use of ZnNPs-As ointments significantly ($P \leq 0.01$) raised the wound contracture, vessel, hydroxyl proline, hexuronic acid, hexosamine, fibrocyte, fibroblast and fibrocytes/fibroblast rates and significantly ($P \leq 0.01$) decreased the wound area, total cells, neutrophil, macrophage and lymphocyte compared to other groups in rats. As per observation, ZnNPs-As may be consumed for the treatment of cutaneous wounds and infectious diseases in humans [32].

Local Anesthetic Applications of ZnO-NPs

Cui *et al.* have reported the biosynthesis of ZnO-NPs by using aqueous extract of *Cinnamon zeylanicum* leaf with $Zn(CH_3COO)_2 \cdot 2H_2O$ as initiator for bioreduction. The reported spherical-shaped NPs of 20 nm size expressed potent local anaesthetic properties. The activity of local anaesthesia was tested in frog models and it was observed that withdrawal reflex of frog's foot time of anaesthesia onset was 8.17, 15.00, 6.5 and 10.50 min at a dosage of 40 mg, 12 mg, 80 mg and 20 mg of the methanolic ZnO-NPs, respectively. ANOVA (one-way analysis of variance) displays that local anaesthetic activity was extremely significant [33].

Bone (Osteo) Applications of ZnO-NPs

Dongyan *et al.* synthesized spherical-shaped ZnO-NPs of 20-nm size from precursor zinc acetate dihydrate by an environmentally friendly approach through an aqueous extract of *Artemisia annua* stem barks. The synthesized NPs have worked as an inhibitor of osteoclast formation related to bone deformities and bone-related diseases. The viability of MG-63 cells

was assayed by MTT test and osteogenic-related assays, like real-time PCR and mineralization assay, were adopted to determine the effects of *A. annua* ZnO-NPs on the multiplication and differentiation of human osteoblast-like MG-63 cells. The synthesized *A. annua* ZnO-NPs enhanced the proliferation, differentiation and mineralization without causing significant cytotoxic impact on MG-63 cells. These effects indicate that *A. annua* ZnO-NPs can both stimulate bone formation *via* the differentiation of MG-63 cells. Hence, it was concluded that *A. Annua* ZnO-NPs can be a promising agent for the treatment of bone deformities and bone-related diseases [34].

Anti-cancer Applications of ZnO-NPs

Duan *et al.* have demonstrated the flora-mediated generation of ZnO-NPs through water and alcoholic extracts of leaves of *Cardiospermum halicacabum*(CH). The NPs of spherical shape and 10-20 nm size expressed promising cytotoxic capacity. The cell adhesion assay showed better adherent results for the time of 24 hr and 12 hr, respectively. *C. halicacabum* ZnO-NPs (12.5 µg/mL) exposed moderate (12 hr incubation) and much adhesion (24 hr incubation) to the adherent cells and the standard doxorubicin (2 µM/mL). The mRNA expression of apoptotic genes like caspase 3, 8 and 9 was elevated followed by the exposure to ZnO nanoparticles and it was narrowly proved that ZnO nanoparticles stimulate the apoptotic cell necrosis at the transcriptional stage. CH-ZnO nanoparticles persuaded programmed cell necrosis *via* elevated ROS levels in cells. CH-ZnO-NPs further stimulates the markers of apoptosis and aggravates necrosis of cancerous cells, toxicity to cells and increase of ROS. With observations, this might accomplished that CH-ZnO-NPs complexed with CH appreciably possessed a toxicity to human melanoma cells (A375) *via* provoking the apoptotic cell necrosis [35].

Zheng *et al.* have revealed interesting facts about the biosynthesis of ZnO-NPs in the presence of an aqueous solution of *Rhizoma paridis* saponins extract with zinc acetate initiator. The results found that spherical-shaped 100nm NPs were produced. The *R. paridis* saponins-based ZnO NPs (RPS-ZnO NPs) have been seen to destroy the mitochondria and cause necrosis of cells by increasing intracellular antioxidant generation. The research revealed that

supplementation of RPS-ZnO NPs changed the morphological linkage with Molt-4 cells, which resulted in the induction of apoptosis [36].

Tang. *et al.* have developed ZnO-NPs of 100 nm size through an eco-friendly process by employing $[Zn(NO_3)_2 \cdot 6H_2O]$ as the precursor along with water extract of leaves of *Morus nigra*(MN). The synthesized spherical-shaped NPs have been reported to exhibit the anticancer effect against AGS cells and were analyzed through cell viability, apoptotic morphological variations by AO/EtBr, alterations of mitochondrial membrane potential (MMP), cell cycle arrest, lipid peroxidation status (TBARS), antioxidants (SOD, GSH and CAT) and generation of ROS. The status of apoptosis genes, such as bax, caspase-9, caspase-3 and Bcl-2 expressions, was analyzed by using RT-PCR techniques. Observation revealed that gastric cancer cells demonstrated cell death by MN-ZnO-NPs treatment. The MN-ZnO-NPs induced apoptosis by enhanced formation of ROS, decreased MMP, increased lipid peroxidation, decreased antioxidants and induced cell cycle arrest, as was observed [37].

Mohammad *et al.* utilized the precursor zinc acetate dihydrate $Zn(CH_3COO)_2 \cdot 2H_2O$ for the synthesis of ZnO-NPs by using aqueous extract of Hyssop (*Hyssopus officinalis*) leaf. The obtained spherical NPs demonstrated impressive anti-cancer activity. The green synthesis of Hy-ZnO-NPs affects PC3 cell line and BALB/c mice model. The cytotoxicity of ZnO-NPs was assessed on PC3 cell line by MTT test and apoptotic effect of ZnO-NPs was determined by *in vitro* AO/PI staining. The expression of major genes involved in spermatogenesis and sperm maturation (Adam3, Prml, Spata19, Tnp2 and Gpx5) was also analyzed. The obtained results showed that the IC₅₀ for PC3 cell line was reported to be 8.07 and 5 µg/ml (24 and 48h). Meanwhile, the induced apoptosis was recorded as 26.6% ± 0.05, 44% ± 0.12 and 80% ± 0.07 of PC3 cells. The percentage of induced apoptosis by ZnO-NPs was reported as 80% apoptosis in PC3 cells treated with 19.53 µg/ml of green-synthesised ZnO-NPs. These results indicated that along with the increment of treatment duration and concentration of green-synthesised ZnO-NPs, apoptosis may increase [38].

Selim *et al.* revealed an interesting biosynthesis approach for ZnO-NPs through an aqueous extract of *Deverra tortuosa* plant by

utilizing $[\text{Zn}(\text{NO}_3)_2 \cdot 6\text{H}_2\text{O}]$ as the precursor. The reported NPs have a spherical shape with a size range of 9.26–31.18 nm. The potential anticancer activity was investigated against two cancer cell lines “Caco-2” and “A549” compared to their activities on the human lung fibroblast cell line (WI38) using the MTT assay. Both the aqueous extract and ZnO-NPs showed a remarkable selective cytotoxicity against the two examined cancer cell lines investigated using doxorubicin as the positive control, and the untreated cells as the negative control. This effect was concentration-dependent, IC_{50} values of A549 cells were 193.12 and 83.47, while IC_{50} values of Caco-2 cells were 136.12 and 50.81 $\mu\text{g}/\text{mL}$ by the extract and ZnO-NPs, respectively. Significantly higher IC_{50} values of 902.83 and 434.60 $\mu\text{g}/\text{mL}$ were obtained from the treatment of the normal lung epithelial cell (WI38) with the respective materials [39].

Nilavukkarasi *et al.* have reported the biosynthesis of ZnO-NPs by using *Capparis zeylanica* leaf extract with zinc acetate dihydrate $[\text{Zn}(\text{CH}_3\text{CO}_2)_2 \cdot 2\text{H}_2\text{O}]$ as an initiator of the reaction. The reported NPs were of spherical-shape and 32–40 nm size. Observation exposed that microbial growth decreases with increase in the concentration of synthesized ZnO-NPs investigated against gram-positive bacteria (*Staphylococcus epidermidis*, *Enterococcus faecalis*), gram-negative bacteria (*Salmonella paratyphi*, *Shigella dysenteriae*) and fungi (*Candida albicans*, *Aspergillus niger*) by well diffusion method. Cytotoxicity of biosynthesized ZnO nanoparticles treated with lung cancer cell line (A549) was analyzed by cell proliferation assay. Synthesized ZnO-NPs could reduce cell viability after 48 h with significant decreases in cell viability at 22% and 38%. The morphological changes of A549 cells were exposed in higher concentrations of treated cells including cell shrinkage and extensive detachment of the cells. Therefore, bio-mediated ZnO nanostructures proved to be an excellent novel antimicrobial and anticancer material [40].

Multiple Applications of ZnO-NPs

Mohamed *et al.* have reported an interesting way of biosynthesizing ZnO-NPs from the aqueous extract of *Hyphaene thebaica* fruit by utilizing zinc acetate dihydrate as the precursor. The synthesized quasi-spherical-shaped NPs of size of 8–23 nm demonstrated dose-dependent promising results against anti-microbial

potential, anti-oxidant potential, anti-leishmanial potential and cytotoxicity dependence. Excellent protein kinase (PK) inhibition and varying antimicrobial potential against different bacterial and fungal strains are reported. *E.coli* and *A.flavus* were found the most susceptible microbial strains. MTT assay revealed an IC_{50} of 106 $\mu\text{g}/\text{mL}$ against *Leishmania tropica*. Antifungal activities of the ZnO-NPs across different test concentrations (4–250 $\mu\text{g}/\text{mL}$) were reported. ZnO-NPs indicated varying antifungal potential against the tested fungal strains. *A. flavus* and *A. niger* revealed highest susceptibility to the nanoparticles (4 mg/mL) and zones of 11.8 mm and 10 mm were obtained, respectively. Excellent protein kinase inhibition potential is reported with the highest zone of inhibition reported as 12 mm at 4 mg/mL and the diameter of the zones gradually declined with the decrease in concentration. Streptomycin control revealed an inhibition zone of 31.5 mm. Different antioxidant assays indicated the antioxidant potential of ZnO-NPs. The DPPH radical scavenging activity was 55% at 400 $\mu\text{g}/\text{mL}$ and 22% at 25 $\mu\text{g}/\text{mL}$. Total antioxidant capacity was recorded as 39.6 μg AAE/mg at 400 $\mu\text{g}/\text{mL}$. The highest value recorded for the reducing power was 79 μg AAE/mg at 400 $\mu\text{g}/\text{mL}$ [41].

Karunakaran *et al.* have synthesized eco-friendly ZnO-NPs by utilizing zinc nitrate hexahydrate $[\text{Zn}(\text{NO}_3)_2 \cdot 6\text{H}_2\text{O}]$ with the help of aqueous extract of flower of *Hylotelephium telephium* subsp. The synthesized NPs have an oval to spherical shape with 83 nm size. The developed NPs have antioxidant (free radical scavenging activity) and anti-pathogenic activity. The percentage of free radicals scavenged by the ZnO-NPs increased with an increase in their masses, exhibiting 18% (1 mg), 35% (5 mg), 50% (10 mg) and 75% (100 mg). The clear zone around the nanoparticles indicates their antibacterial activity against the tested bacteria *S.aureus* and *K.pneumoniae*. Streptomycin was used as a standard. The ZnO-NPs showed 16 ± 0.24 mm and 14 ± 0.38 mm, respectively. The antibacterial activity of the tested nanoparticles might be due to their interaction with the peptidoglycan layer mediated by electrostatic interaction [42].

Jayappa *et al.* have reported the biosynthesis of ZnO-NPs by employing the air-dried leaves of *Mussaenda frondosa* extract with zinc nitrate

hexahydrate $[Zn(NO_3)_2 \cdot 6H_2O]$ as the initiator for developing NPs. The spherical-shaped ZnO-NPs had a 5-20 nm size. The ZnO-NPs expressed exceptional pharmacological activities, like anti-diabetic, anti-oxidant, anti-cancer and anti-microbial activities. The IC_{50} values of ZnO-NPs for quenching DPPH radical was found to be 824 $\mu\text{g/ml}$ (L-ZnO-NP), 752 $\mu\text{g/ml}$ (S-ZnO-NP) and 857 $\mu\text{g/ml}$ (C-ZnO-NP). The S-ZnO-NPs (from stem) exhibited effective antioxidant activity compared to L-ZnONP (from leaf) and C-ZnO-NP (from callus). It was observed that all the ZnO-NPs showed inhibition against all the tested strains except for *P.vulgaris*. Among the tested strains, *E.coli* was found to be more susceptible to S-ZnO-NPs with 28.64 mm zone of inhibition ($p < 0.05$) compared to the standard. The highest mean zone of inhibition observed against *P.aeruginosa*, *S.aureus* and *B.subtilis* was found to be 20.31 mm (S-ZnO-NP), 21.51 mm (C-ZnO-NP) and 19.13 mm (S-ZnO-NP), respectively at $P < 0.05$. Highly significant MIC was recorded against *E.coli* at 19.23 $\mu\text{g/ml}$ with $P < 0.05$, which was followed by the activity against *P.aeruginosa*, *S.aureus* and *B.Subtilis*, showing MIC values of 35.46, 54.13 and 93.14 $\mu\text{g/ml}$. as compared with MIC values of the standard (8.44 to 22.13 $\mu\text{g/ml}$) [43].

Dhandapani *et al.* revealed the biosynthesis of ZnO-NPs through an aqueous extract of *Melia azedarach* leaf by utilizing $[Zn(NO_3)_2 \cdot 6H_2O]$ as the precursor. The synthesized spherical-shaped NPs of 33-96 nm size represented promising anti-oxidant and anti-bacterial properties. ZnO-NPs and *M.azedarach* aqueous leaf extract revealed divergent levels of superoxide anion radical scavenging activity in the ranges between 25, 50, 100, 150, 200 $\mu\text{g/mL}$ concentrations compared with the standard Butylated Hydroxyl Toluene (BHT). Superoxide anion radical scavenging activity of ZnO-NPs shows 27.58%, 37.40%, 43.93%, 48.07% and 52.28% compared with the standard BHT exhibiting 34.82%, 37.08%, 46.78%, 55.10% and 58.92% of hydroxyl radical scavenging activity [44].

Vidhya *et al.* reported an environmentally friendly way of synthesis of spherical-shaped ZnO-NPs of 45 nm size by using *O.americanum* leaf extract with $Zn(CH_3COO)_2 \cdot 2H_2O$ as the initiator of the reaction. The novel ZnO nanomaterials displayed bacteriocidal, fungicidal and anti-proliferative activity against human skin cancer cell line. Bio-inspired ZnO-NPs have

performed activity against skin disease-causing pathogens, such as *B.cereus*, *C.penfringens*, *K.pneumoniae*, *S.paratyphi*, *C.albicans* and *A.niger*, resulting in that ZnO-NPs displayed excellent antimicrobial activity with the highest inhibition zone with *C.penfringens* (30 mm), followed by *K.pneumoniae* (27 mm), *B.cereus* (25 mm) and *S.paratyphi* (24 mm). The antifungal activity with ZnO-NPs shows a maximum zone of inhibition with *C.albicans* (28 mm), followed by *A.niger* (24 mm). The nanoparticles can enter the microbial cell membrane due to immediate electrostatic interactions formed at the interface to release reactive oxygen species to promote cell damage [45].

Eaton *et al.* revealed an interesting fact about the biosynthesis of ZnO- NPs from the precursor $[Zn(NO_3)_2 \cdot 6H_2O]$ using the aqueous extract of *Melia azedarach* leaf. The synthesized spherical-shaped NPs have a size range of 35-129 nm. ZnO-NPs presented significant inhibition towards yeasts of the genus *Candida*, particularly *Candida parapsilosis* which is an important emerging pathogen, with no toxicity against red blood cells, which indicates a promising material that could be safely used in medical devices or in pharmaceutical formulations as a support to antifungal treatments. In terms of antifungal activity at different concentrations tested, bulk ZnO exhibited inhibition of *C.krusei*, only at the high concentration of 1,000 $\mu\text{g/mL}$. On the other hand, the ZnO-NPs synthesized showed improved antifungal potential against yeasts, demonstrating that ZnO-NPs improve their antifungal capacity at lower concentrations [46].

Abbasi *et al.* synthesized spherical ZnO-NPs of 18 nm size from the aqueous extract of *Geranium wallichianum* leaves with the precursor zinc nitrate hexahydrate $[Zn(NO_3)_2 \cdot 6H_2O]$. The fabricated NPs showed anti-pathogenic potentials, free radical scavenger capacities and inhibition of α -amylase and protein kinases. Antileishmanial potential of ZnO-NPs was evaluated using *L.tropica* (KMH23) parasites which were evaluated at various doses (1–200 $\mu\text{g/mL}$) of ZnO-NPs. ZnO-NPs showed a significant antileishmanial potential against *L.tropica* promastigotes with IC_{50} of 15.60 $\mu\text{g/mL}$. Similarly, ZnO-NPs also showed a significant potential against *L.tropica* amastigotes with IC_{50} of 34.5 $\mu\text{g/mL}$. Fungicidal potential of ZnO-NPs was evaluated using

various fungal strains (FS) compared with drug amp-B as a positive control. A dose-dependent inhibition response was reported. *A.flavus* was the least susceptible fungal strain with MIC of 250 µg/mL, while *A.niger* and *M.racemosus* were the most susceptible strains with MIC of 31.25 µg/mL. The PK inhibition activity was tested using different doses of ZnO-NPs ranging from 31.25-1000 µg/mL. The highest ZOI was measured as 15 mm at 1000 µg/mL, which shows an important protein kinase inhibition potency of ZnO-NPs compared with surfactin as a positive control [47].

Miri *et al.* have studied the interesting facts of developing ZnO-NPs from the aqua extract of *Prosopis farcta* fruit by utilizing zinc sulfate as the precursor. These NPs have a spherical shape with a size range of 40-50 nm. The produced NPs showed better antifungal activity and inhibition of breast cancer proliferation as compared to the ionic form. The MIC and MFC of ZnO-NPs against *C.albicans* have been surveyed *via* turbidimetric antifungal assay and calculated to be 32–64 and 128–512 µg/ml, respectively. Results showed that ZnO-NPs possess a good antifungal activity against *C.albicans*. Then, cytotoxic activity of synthesized NPs was evaluated by using WST-1 assay on MCF7 cell line. Cell viability of synthesized NPs was observed to be 50.23% at 500 µg/ml concentration of NPs [48].

Sarlia *et al.* studied the potentials of ZnO-NPs developed from the aqueous extract of leaves, trunks and shells of *Taxus baccata* plant by utilizing $[Zn(NO_3)_2 \cdot 6H_2O]$ as the precursor. The reported NPs had a spherical shape with 60-80 nm size, resulting in promising anti-bacterial activity. The antimicrobial activities of the *Taxus baccata* extract, zinc nitrate solution and Zn nanoparticles (Zn-NPs) were examined by the well diffusion method. The extract and solution did not show antimicrobial effects against *Staphylococcus aureus*, *Escherichia coli* and *Pseudomonas aeruginosa*. In negative control wells, no bacterium was grown, while in positive control wells, a very good growth of bacteria was observed [49].

Hemanth *et al.* have fabricated an environmentally benign method to synthesize

(aqueous extract of *Simarouba glauca* DC leaves)-based hexagonal ZnO-NPs of size range 17-37 nm by utilizing $Zn(NO_3)_2 \cdot 6H_2O$ salt as the precursor. The antioxidant potential of the synthesized ZnO-NPs was estimated by DPPH, ABTS, H_2O_2 and superoxide radical scavenging methods. The RSA of ZnO-NPs was found between 5 and 59% (among different methods) and the antioxidant potential increased with increase in the concentration of ZnO-NPs. The half-maximal inhibitory concentration (IC_{50}) of RSA varied between 400 and 500 µg mL⁻¹ among the test methods. The standard control (ascorbic acid) offered 75% inhibition at 50 µg mL⁻¹. The antimutagenic activity of green synthesized ZnO-NPs was studied using allium assay. Onion is considered as a good bioindicator for genotoxicity and clastogenicity studies by UNEP and USEPA. In this study, the mitotic index was decreased from 43.06 to 17.46% with an increase in the concentration of ZnO-NPs compared to the control [50].

Narain *et al.* have produced eco-friendly approach-mediated spherical ZnO-NPs of an average size of 81 nm from *Phoenix loureiroi* aqueous fruit by using zinc nitrate hexahydrate $[Zn(NO_3)_2 \cdot 6H_2O]$ as the precursor. The antioxidant and cytotoxic properties were investigated in the biologically and chemically synthesized zinc oxide (ZnO)-B and chitosan (CTS)-encapsulated ZnO (ZnO-CTS) nanoparticles. The synthesized (B-ZnO and B-ZnO-CTS) nanoparticles showed higher free radical scavenging ability in DPPH (IC_{50} = 445.94 and 419.32 µg/mL), ABTS (37.95 and 45.61%), NO (20.52 and 21.28%) and OH· (74.09 and 77.10%) assays. Hemolytic test was performed by using RBCs *in vitro* for the study of interaction of fruit extract and nanoparticles with membranes, because this test is a good indicator of destruction of RBC cells. The results showed that the gradual increase of hemolytic activity (0.65–1.43%) was in a dose-dependent manner in methanolic extracts. Results showed that C-ZnO nanoparticles have a higher percentage (7.85%) of hemolysis at 2.50 mg/mL. Thus, up to 1.50 mg/mL concentration, the nanomaterial can be used as a biocompatible material [51].

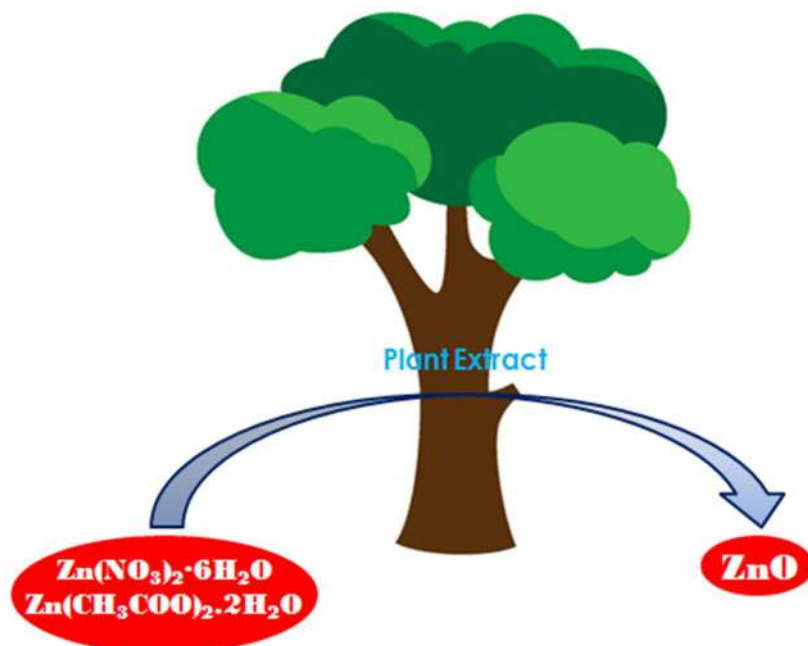


FIG. 1. Fabrication of zinc nanomaterials from various zinc salts employing different plant extracts.

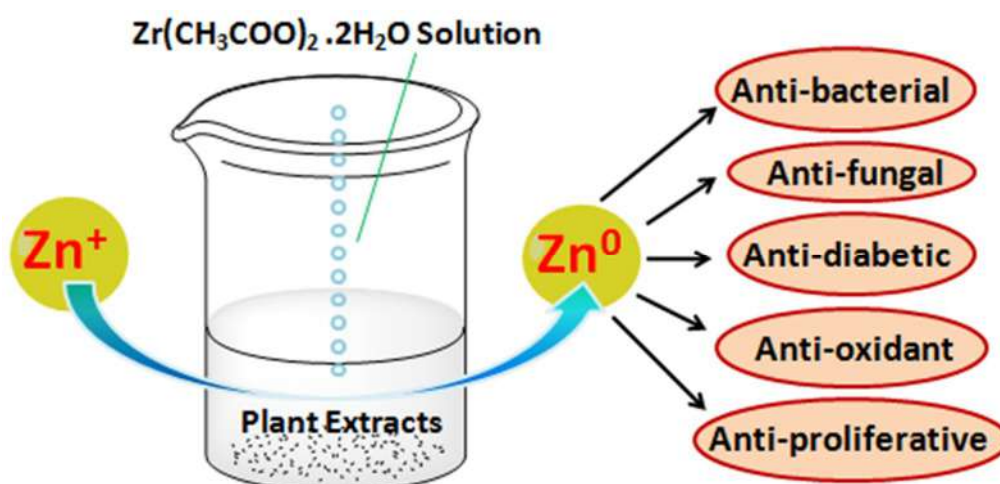


FIG. 2. Zinc nanomaterials formation from different plant extracts and their pharmacotherapeutics.

TABLE 1. Fabrication of zinc nanomaterials through various plant biomasses.

Plant	Family	Part used	Average size (nm)	Shape	Therapeutic applications	Precursor	Reference
<i>Sesamum indicum</i>	Pedaliaceae	seeds	9.07	Spherical	Anti-bacterial	ZnSO ₄ ·7H ₂ O	[17]
<i>Echinochloa frumentacea</i> grains	Poaceae	grain	35-65	Hexagonal shape	Anti-bacterial	Zn(CH ₃ COO) ₂ ·2H ₂ O	[18]
<i>Euphorbia hirta</i>	Euphorbiaceae	leaf	20-25	Spherical shape	Anti-microbial	Zinc nitrate	[19]
radish root (<i>Raphanussativus</i>) extract	Brassicaceae	root	15-25	Hexagonal structure	Dressing agents for diabetic foot ulcers	Zn(CH ₃ COO) ₂ ·2H ₂ O	[20]
<i>Aloe socotrina</i>	Asphodelaceae	leaf	15-50	Spherical	Anti-bacterial	Zn(CH ₃ COO) ₂ ·2H ₂ O	[21]
<i>Camellia japonica</i>	Theaceae	leaf	15-30	Spherical shape	Anti-bacterial, Anti-fungal	Zn(NO ₃) ₂ ·6H ₂ O	[22]
<i>Aloe vera</i>	Asphodelaceae	leaf	18-61	Rod shape	Anti-bacterial	Zinc nitrate	[23]

Natural Extracts-mediated Biosynthesis of Zinc Oxide Nanoparticles and Their Multiple Pharmacotherapeutic Perspectives

Plant	Family	Part used	Average size (nm)	Shape	Therapeutic applications	Precursor	Reference
<i>Prosopis juliflora</i>	Leguminosae	leaf	65	Spherical shape	Anti-bacterial	Zn(NO ₃) ₂ ·6H ₂ O	[24]
Plum fruits	Rosaceae	fruit	60-80	Cylindrical	Anti-bacterial	Zn(CH ₃ COO) ₂ ·2H ₂ O	[25]
<i>Ailanthus altissima</i>	Simaroubaceae	fruits	5-18	Spherical shape	Anti-bacterial	Zn(NO ₃) ₂ ·6H ₂ O	[26]
<i>Cinnamomum verum J. Presl</i>	Lauraceae	bark	~45	Spherical	Anti-bacterial	Zn(NO ₃) ₂ ·6H ₂ O	[27]
<i>Eucalyptus globules</i>	Myrtaceae	leaf	52-70	Spherical	Anti-fungal	Zn(NO ₃) ₂ ·6H ₂ O	[28]
Nettle (<i>Urtica dioica</i>)	Urticaceae	leaf	NA	NA	Anti-diabetic	Zn(NO ₃) ₂ ·6H ₂ O	[29]
<i>Selaginella convolute</i>	Selaginellaceae	leaf	40	Spherical	Muscle relaxant, Anti-nociceptive	Zn(CH ₃ COO) ₂ ·2H ₂ O	[30]
<i>Fraxinus rhynchophylla</i>	Oleaceae	wood	100-200	NA	Anti-nociceptive	Zn(CH ₃ COO) ₂ ·2H ₂ O	[31]
<i>Allium sar alicum R.M. Fritsch</i>	Amaryllidaceae	leaf	19	Spherical	Anti-oxidant, Anti-bacterial, Anti-fungal	[Zn(NO ₃) ₂ ·6H ₂ O]	[32]
<i>Cinnamon zeylanicum</i>	Lauraceae	leaf	20	Spherical shape	Local anaesthetics	Zn(CH ₃ COO) ₂ ·2H ₂ O	[33]
<i>Artemisia annua</i>	Asteraceae	stem, bark	20	Spherical shape	Inhibition of osteoclast formation, Treatment of bone deformities and bone-related diseases	Zn(CH ₃ COO) ₂ ·2H ₂ O	[34]
<i>Cardiospermum halicacabum</i>	Sapindaceae	leaf	10-20	Spherical shape	Anti-cancer activity in human melanoma cells (A375)	Zn(CH ₃ COO) ₂ ·2H ₂ O	[35]
<i>Rhizoma paridis saponins</i>	Liliaceae	leaf	100	Spherical shape	Anti-carcinogenic	Zn(CH ₃ COO) ₂ ·2H ₂ O	[36]
<i>Morus nigra</i>	Moraceae	leaf	100	Spherical shape	Anti-cancer, gastric cancer	Zn(NO ₃) ₂ ·6H ₂ O	[37]
<i>Hyssop (Hyssopus officinalis)</i>	Lamiaceae	leaf	NA	NA	Anti-cancer	Zn(CH ₃ COO) ₂ ·2H ₂ O	[38]
<i>Deverra tortuosa extract</i>	Apiaceae	aerial parts	9.26-31.18	Spherical shape	Anti-microbial, Anti-cancer	Zn(NO ₃) ₂ ·6H ₂ O	[39]
<i>Capparis zeylanica</i>	Capparaceae	leaf	32-40	Spherical sizes	Anti-proliferative, Anti-cancer	Zn(CH ₃ COO) ₂ ·2H ₂ O	[40]
<i>Hyphaene thebaica</i>	Arecaceae	fruit	8-23	Quasi-spherical	Anti-microbial, Anti-leishmanial	Zn(CH ₃ COO) ₂ ·2H ₂ O	[41]
<i>Hylotelephium telephium subsp.</i>	Crassulaceae	flower	83 nm	Spherical	Anti-bacterial	[Zn(NO ₃) ₂ ·6H ₂ O]	[42]
<i>Mussaenda frondosa</i>	Rubiaceae	leaf, stem and callus	5-20	Spherical	Anti-oxidant, Anti-inflammatory, Anti-diabetic, Antimicrobial, Anti-cancer	Zn(NO ₃) ₂ ·6H ₂ O	[43]
<i>Melia azedarach</i>	Meliaceae	leaf	33-96	Spherical shape	Anti-oxidant, Anti-bacterial	Zn(NO ₃) ₂ ·6H ₂ O	[44]
<i>Ocimum americanum</i>	Lamiaceae	leaf	45	Spherical shape	Anti-microbial, Anti-cancer	Zn(CH ₃ COO) ₂ ·2H ₂ O	[45]
Cashew Gum	Anacardiaceae	gum	35-129	Round-shaped	Anti-fungal	Zn(NO ₃) ₂ ·6H ₂ O	[46]
<i>Geranium wallichianum</i>	Geraniaceae	leaf	~18	Spherical	Anti-cancer, Anti-leishmanial	Zn(NO ₃) ₂ ·6H ₂ O	[47]
<i>P. farcta</i>	Fabaceae	fruit	40-50	Hexagonal	Anti-microbial	ZnSO ₄	[48]

Plant	Family	Part used	Average size (nm)	Shape	Therapeutic applications	Precursor	Reference
<i>Taxus baccata</i>	Taxaceae	leaves, trunks and shells	20-27	Hexagonal	Anti-bacterial, Anti-cancer	Zn(NO ₃) ₂ ·6H ₂ O	[49]
<i>Simarouba glauca</i>	Simaroubaceae	leaf	17-37	Hexagonal	Anti-oxidant, Anti-mitotic	Zn(NO ₃) ₂ ·6H ₂ O	[50]
<i>Phoenix loureiroi</i> fruit	Arecaceae	fruit	81	Spherical shape	Anti-oxidant, Anti-cancer	Zn(NO ₃) ₂ ·6H ₂ O	[51]

Conclusion

This article provided information to active researchers on the recent advances in the area of zinc oxide (ZnO) nanoparticles development of diverse morphologies (hexagonal, spherical, quasi-spherical, rod, cylindrical, ... etc.) from various precursor zinc salts [Zn(NO₃)₂·6H₂O, Zn(CH₃COO)₂·2H₂O and ZnSO₄] using the extracts of plant parts (leaf, stem, bark, fruit, flower, seed, wood, trunk and grain). The pharmacological perspectives of these

nanomaterials, such as anti-oxidant, anti-inflammatory, anti-leishmanial, anti-diabetic, anti-bacterial, anti-fungal, anti-cancer, local anaesthetic, muscle relaxant, anti-nociceptive, dressing agents, osteoclast formation inhibitor, ... etc., have opened new avenues of therapeutic applications. This literature opened new future perspectives for researchers in developing zinc-based nanomaterials which will have multifarious applications.

References

- [1] Marcelo, G.A. *et al.*, Mater. Sci. Eng. C, 106 (2020) 110104.
- [2] Choudhury, H. *et al.*, Mater. Sci. Eng. C, 112 (2020) 110925.
- [3] Chandra, H. *et al.*, Biocatal. Agric. Biotechnol., 24 (2020) 101518.
- [4] Bandeira, M. *et al.*, Sustain. Chem. Pharm., 15 (2020) 100223.
- [5] Gu, M. *et al.*, Chem. Phys., 534 (2020) 110750.
- [6] Hu, H. *et al.*, J. Hazard. Mater., 387 (2020) 121670.
- [7] Sachdeva, A. *et al.*, Mater. Today Proc., (2020) in Press.
- [8] Bhattacharya, P. *et al.*, J. Environ. Chem. Eng., 8 (3) (2020) 103803.
- [9] Chandra, N. *et al.*, Groundw. Sustain. Dev., 10 (2020) 100325.
- [10] Chakrabarti, S., Banerjee, P., Mitra, P. and Roy, A., "Zinc Oxide-based Nanomaterials for Environmental Applications". (Elsevier, 2020).
- [11] Pillai, A.M. *et al.*, J. Mol. Struct., 1211 (2020) 128107.
- [12] Nasrollahzadeh, M., Sajadi, S.M., Issaabadi, Z. and Sajjadi, M., "Biological Sources Used in Green Nanotechnology", 1st Ed., vol. 28, (Elsevier, 2019).
- [13] Jose Varghese, R., Zikalala, N., Sakho, E.H.M. and Oluwafemi O.S., "Green Synthesis Protocol on Metal Oxide Nanoparticles Using Plant Extracts", (Elsevier, 2020).
- [14] Shrivastava, M. *et al.*, Environ. Nanotechnology, Monit. Manag., 11 (2019) 100218.
- [15] Das, G. *et al.*, Mater. Sci. Eng. C, 114 (2020) 111011.
- [16] Alharbi, F.A. and Alarfaj, A.A., J. King Saud Univ. Sci., 32 (2) (2020) 1346.
- [17] Zafar, S. *et al.*, J. King Saud Univ. Sci., 32 (1) (2020) 1116.
- [18] Velsankar, K. *et al.*, Mater. Chem. Phys., 239 (2020) 121976.
- [19] Ahmad, W. and Kalra, D., J. King Saud Univ. Sci., 32 (4) (2020) 2358.
- [20] Liu, D. *et al.*, J. Drug Deliv. Sci. Technol., 55(23) (2020) 101364.
- [21] Fahimmunisha, B.A. *et al.*, J. Drug Deliv. Sci. Technol., 55 (2020) 101465.

- [22] Muthuchamy, M. *et al.*, *Mater. Today Commun.*, 22 (2020) 100766.
- [23] Rasli, N.I. *et al.*, *Heliyon*, 6 (1) (2020) e03156.
- [24] Sheik Mydeen, S. *et al.*, *J. Saudi Chem. Soc.*, 24 (5) (2020) 393.
- [25] Singhal, U. *et al.*, *Mater. Today Proc.*, 28 (1) (2020) 261.
- [26] Awwad, A.M. *et al.*, *Chem. Int.*, 6 (3) (2020) 15.
- [27] Ansari, M.A. *et al.*, *Biomolecules*, 10 (2) (2020) 1.
- [28] Ahmad, H. *et al.*, *Biomolecules*, 10 (3) (2020) 1.
- [29] Bayrami, A. *et al.*, *Adv. Powder Technol.*, 31 (5) (2020) 2110.
- [30] Xu, K. *et al.*, *J. Photochem. Photobiol. B Biol.*, 202 (2020) 111700.
- [31] Wang, Z. *et al.*, *J. Photochem. Photobiol. B Biol.*, 202 (2020) 111668.
- [32] Zhang, C. *et al.*, *Appl. Organomet. Chem.*, 34 (2020) e5564.
- [33] Cui, P. *et al.*, *J. Drug Deliv. Sci. Technol.*, 57 (29) (2020) 101740.
- [34] Wang, D. *et al.*, *J. Photochem. Photobiol. B Biol.*, 202 (2020) 111652.
- [35] Duan, X. *et al.*, *J. Photochem. Photobiol. B Biol.*, 202 (2020) 111718.
- [36] Xu, Z. *et al.*, *J. King Saud Univ. Sci.*, 32 (3) (2020) 1865.
- [37] Tang, Q. *et al.*, *J. Photochem. Photobiol. B Biol.*, 202 (2020) 111698.
- [38] Mohammad, G.R.K.S. *et al.*, *Andrologia*, 52 (1) (2020) e13450.
- [39] Selim, Y.A. *et al.*, *Sci. Rep.*, 10(1) (2020) 1.
- [40] Nilavukkarasi, M. *et al.*, *Mater. Sci. Energy Technol.*, 3 (2020) 335.
- [41] Mohamed, H.E.A. *et al.*, *J. Inorg. Organomet. Polym. Mater.*, 30 (2020) 3241.
- [42] Karunakaran, G. *et al.*, *Jom*, 72 (3) (2020) 1264.
- [43] Jayappa, M.D. *et al.*, *Appl. Nanosci.*, 10 (2020) 3057.
- [44] Dhandapani, K.V. *et al.*, *Biocatal. Agric. Biotechnol.*, 24 (2020) 101517.
- [45] Vidhya, E. *et al.*, *Gene Reports*, 20 (2020) 100688.
- [46] Souza, J.M.T. *et al.*, *J. Clean Prod.*, 247 (2020) 119085.
- [47] Abbasi, B.A. *et al.*, *Biomolecules*, 10 (1) (2020) 1.
- [48] Miri, A. *et al.*, *Green Chem. Lett. Rev.*, 13 (1) (2020) 27.
- [49] Sarli, S. *et al.*, *Eurasian Chem. Commun.*, 2 (3) (2020) 302.
- [50] Hemanth Kumar, N.K. *et al.*, *J. Clust. Sci.*, 31 (2) (2020) 523.
- [51] Narain, M. *et al.*, *Arab. J. Sci. Eng.*, 45 (1) (2020) 15.